European Journal of Ophthalmology / Vol. 16 no. 2, 2006 / pp. 251-258

Glaucoma detection using the GDx nerve fiber analyzer and the retinal thickness analyzer (RTA)

E.M. HOFFMANN[1,2], C. BOWD[2], N. KLEIN[1], K. STEMBERGER[1], F.H. GRUS[1], N. PFEIFFER[1]

[1]Universitäts-Augenklinik, Mainz - Germany
[2]Hamilton Glaucoma Center, University of California, San Diego - USA

PURPOSE. *To compare the ability of the nerve fiber analyzer (GDx) and the retinal thickness analyzer (RTA) to discriminate between glaucomatous and healthy eyes.*
METHODS. *Thirty-seven glaucoma patients (early to moderate severity) and 34 healthy controls were included. Glaucoma patients were defined as those with two repeatable abnormal visual fields by automated perimetry within 1 year. All subjects were examined with a GDx scanning laser polarimeter and RTA. Twelve GDx retinal nerve fiber layer parameters and 12 RTA optic disk topography parameters were obtained. GDx and RTA measurements were compared between both experimental groups using t-tests. Areas under the receiver operating characteristic curves (AUROC) for discriminating between healthy and glaucomatous eyes using GDx and RTA parameters were calculated and compared, and sensitivities at ≥80% and ≥95% specificity were reported.*
RESULTS. *Statistically significant differences between glaucomatous and healthy eyes were found for most GDx and RTA parameters. For GDx, the parameter with the largest AUROC for discriminating between healthy and glaucomatous eyes was the number (AUROC = 0.91, sensitivity = 85% at specificity = 84%, sensitivity = 73% at specificity = 95%). For RTA, the parameter with the largest AUROC was mean cup depth (AUROC = 0.79, sensitivity = 61% at specificity = 82%, sensitivity = 33% at specificity = 95%). The AUROC for the GDx number was significantly larger than the AUROC for RTA mean cup depth ($p<0.05$).*
CONCLUSIONS. *GDx showed better discrimination and better sensitivities at fixed specificities than RTA. The currently available RTA optic disk analysis software likely cannot replace GDx RNFL analysis software for successful glaucoma diagnosis. (Eur J Ophthalmol 2006; 16:251-58)*

KEY WORDS. *Glaucoma, Nerve fiber analyzer, Optic nerve imaging, Retinal thickness analyzer*

Accepted: November 15, 2005

INTRODUCTION

The importance of early and objective diagnosis of glaucoma is evident. In the last decade, optical imaging devices have been developed to quantify structural characteristics of the optic nerve head, retinal nerve fiber layer (RNFL), and retina in an attempt to objectively identify glaucoma (1-8).

The recently introduced retinal thickness analyzer (RTA) (6-8) was developed as a competitor to other already well-established imaging devices, such as the GDx nerve fiber analyzer (9-11), to aid in the diagnosis of glaucoma (12-14). To date, no published study has evaluated glaucoma detection using RTA optic disk measurements or compared RTA optic disk measurements and RNFL measurements using GDx for discriminating between healthy and glaucomatous eyes. The purpose of this study was to evaluate and determine the diagnostic accuracy of the RTA compared to the GDx in glaucomatous and healthy eyes.

1120-6721/251-08$15.00/0

METHODS

Subjects

Seventy-one randomly chosen eyes from 71 subjects recruited consecutively from the Glaucoma Unit of the Department of Ophthalmology, University of Mainz, Germany, were included.

Thirty-seven patients had open angle glaucoma (OAG, defined below) and 34 participants served as healthy controls. Subjects included in the study had best-corrected visual acuity (BCVA) of 20/40 or better, a spherical refraction within ±5.0 D and cylinder ±3.0 D, clear media, and were at least 20 years of age.

All patients underwent a complete ophthalmologic assessment including determination of BCVA, slit-lamp biomicroscopy, gonioscopy, stereophotography of the optic disk, automated visual field testing, intraocular pressure (IOP) measurement with Goldmann applanation tonometry in a repeated 24-hour IOP measurement design, pachymetry (DGH 500 Pachette, DGH Technology Inc., Exton), and dilated fundus examination.

The optic nerve head was assessed by a 90- or 78-diopter (D) lens.

Visual field testing was performed using the Octopus 101, V 3.16e (Haag-Streit, Interzeag AG, Switzerland).

Patients were only included if they had reliable visual fields with less than 25% false-positive errors, and less than 25% false-negative errors. A dynamic testing strategy was performed with white Goldmann size III stimuli presented on a 4 apostilb background.

Visual field indices were used to assess the severity of glaucoma according to Flammer et al (15) and Brusini using the Brusini Glaucoma Staging System (GSS) (16).

This system is based on the indices mean deviation (MD) and corrected loss variance (CLV) and classifies visual field defects into five stages. Normal Octopus perimetry results according to the GSS are ±2 dB MD and <4 dB^2 for CLV (17).

GSS Stage 1 represents early, subtle glaucomatous visual field loss; stages 2 and 3 represent moderate visual field loss; and stages 4 and 5 represent advanced visual field loss (18).

No patients with advanced glaucoma were included in the current study. Inclusion and exclusion criteria for the experimental groups are summarized below.

This study adhered to the Declaration of Helsinki, and informed written consent was obtained from all participants.

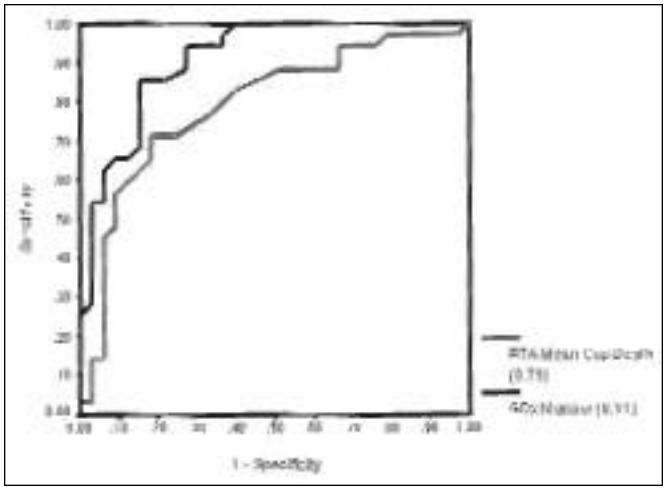

Fig. 1 - *Area under the receiver operating characteristic curves for the best parameter of GDx nerve fiber analyzer (the number) and the retinal thickness analyzer (mean cup depth).*

Criteria for open angle glaucoma

Patients with OAG had open anterior chamber angles and no goniodysgenesis confirmed by gonioscopy, in addition to glaucomatous optic neuropathy (GON) based on both slit-lamp funduscopy and evaluation of stereophotographs of the optic nerve head. GON was defined based on the presence of neuroretinal rim thinning, notching, excavation, nerve fiber layer defects, and/or localized pallor indicative of glaucoma. Patients with type beta peripapillary atrophy were excluded. At least two consecutive abnormal visual fields also were required (Brusini Stage 1–3).

Criteria for healthy subjects

Healthy subjects had no family history of glaucoma, no history of diabetes or other systemic diseases, normal appearing disks on examination, and two normal visual field test results (see criteria above).

Instrumentation

Scanning laser polarimetry. RNFL thickness was measured by scanning laser polarimetry (GDx Nerve Fiber Analyzer, Laser Diagnostic Technologies, San Diego, CA, USA) using a confocal scanning laser ophthalmoscope (wavelength 780 nm) with an integrated polarimeter and fixed corneal polarization compensator. Briefly, the shift (i.e., retardation), caused by the birefringent nature of RNFL microtubules, of polarized light reflected from the reti-

na is assumed to be linearly related to RNFL thickness. The light beam is directed sequentially over each of 256 x 256 peripapillary locations to obtain a thickness map based on the corresponding retardation value at each location. The time to acquire these 65,536 pixel measurements is about 0.7 seconds. At least three images of high quality (passed by software-based image quality assessment and visual assessment by an experienced glaucoma specialist) were acquired using a field of view of 15x15 degrees, and a baseline retardation map was constructed for analysis by creating a mean image of these three measurements. High quality images required good focus and centering with even and appropriate illumination (i.e., not under- or overexposed). Images with 90° shifted RNFL retardation pattern (suggesting inappropriate corneal compensation) were excluded. The GDx Nerve Fiber Analyzer used in this study (software version 3.1) uses a fixed anterior segment compensator to neutralize the birefringence of the cornea and the lens (assumed slow axis of corneal polarization of 15 degrees nasally downwards with a magnitude of 60 nm). Neither pupil dilatation nor corneal contact is required. The GDx parameters investigated are listed in Table I.

Retinal thickness analysis. The Retinal Thickness Analyzer (RTA; Talia Visionary Diagnostics, Neve-Ilan, Israel) is a digitized laser slit lamp that uses a helium-neon laser (wavelength 543 nm) as a light source. The RTA used in this study projected a 2 mm laser slit beam obliquely onto the retina in one brief scan. Each scan obtained 10 optical cross-sections, 100 µm wide and 200 µm apart. The area

TABLE I - DESCRIPTION OF GDx PARAMETERS

Number	Neural network number that indicates the likelihood that glaucoma is present (0–30 normal, 30–70 borderline, 70–100 glaucoma)
Symmetry	Ratio of the average of the 1500 thickest pixels in the superior region over the average of the 1500 thickest pixels in the inferior region
Superior ratio	Ratio of the average of the 1500 thickest pixels in the superior region over the average of the 1500 median pixels in the temporal region
Inferior ratio	Ratio of the average of the 1500 thickest pixels in the inferior region over the average of the 1500 median pixels in the temporal region
Superior/nasal	Ratio of the average of the 1500 thickest pixels in the superior region over the average of the 1500 median pixels in the nasal region
Max. modulation	The difference between the thickest and thinnest measurements within the image
Ellipse modulation	Indication of the difference between the thickest parts of the nerve fiber layer and the thinnest parts. Uses the pixels covered by surrounding the optic nerve
Average thickness (µm)	Average thickness for all usable pixels outside the user-defined ellipse and divided by the number of pixels used
Ellipse average (µm)	Average thickness for the pixels along the measuring ellipse
Superior average (µm)	Average thickness for the pixels in the superior quadrant of the measuring ellipse
Inferior average (µm)	Average thickness for the pixels in the inferior quadrant of the measuring ellipse
Superior integral (mm^2)	The total area under the curve (or total volume) of the nerve fiber layer beneath the superior portion of the ellipse surrounding the optic nerve

TABLE II - DESCRIPTION OF RTA PARAMETERS

Disk area (mm^2)	Total area of the disk delimited by the operator-defined contour line
Cup area (mm^2)	Total cup area within the contour line
Cup/disk area ratio	The ratio between the cup area and the disk area, presented as coefficient
Rim area (mm^2)	Total rim area above the reference plane and within the contour line
Cup volume (mm^3)	The volume of the optic disk underneath the reference plane
Rim volume (mm^3)	The volume of the rim area above the reference plane enclosed by the contour line
Mean cup depth (mm)	The mean value of all calculated depths inside the cup area
Maximum cup depth (mm)	The maximum calculated cup depth
Cup shape measure	The disk's slope distribution measurement (negative values represent a mild slope; positive values represent steep slopes)
Height variation contour (mm)	The distance between the lowest and the highest point of the contour line
Mean RNFL thickness (mm)	The mean height of the retinal surface along the contour line and above the reference plane
RNFL cross section area (mm^2)	The mean retinal nerve fiber layer thickness multiplied by the length of the contour line

of one scan is 2x2 mm and the measurement is obtained in 0.3 seconds. Interpolation is used to depict a continuous surface. Recently developed software enables the creation of a three-dimensional topographic map of the optic nerve head for glaucoma diagnosis (software version 3.0). We chose to investigate optic disk topography using the RTA because this software was specifically designed for glaucoma diagnosis.

To define optic disk topography, four overlapping images in the superior, inferotemporal, inferonasal, and temporal areas were performed for each measurement.

Stereometric optic disk parameters and a classification analysis provided by the RTA, some of which rely on the contour line, are similar to those provided by the Heidelberg Retina Tomograph (HRT). RTA images were obtained by a glaucoma specialist. Twenty minutes before the measurements were taken, the pupil was dilated with 0.5% tropicamide and 5% Neo-Synephrine eye drops.

Prior to the topographic disk analysis, a contour line around the optic nerve head was placed using the inner edge of Elschnig's scleral ring while viewing stereophotographs of the optic disk. All images were reviewed for quality by evaluating clarity and even illumination and optic nerve head centering.

The software provides the analysis of 12 disk parameters, presented in color-coded, two- and three- dimensional topographic maps. The parameters and definitions are shown in Table II.

Statistical analyses

T-tests were used to evaluate the differences in GDx and RTA measurements between experimental groups. After Bonferroni correction for multiple comparisons, a p value of no more than 0.002 was considered statistically significant. The areas under receiver operator characteristics curves (AUROC) were used to describe the ability of each parameter from both instruments to differentiate between glaucoma and healthy eyes. The AUROC shows the trade-off between sensitivity and 1 – specificity. An area under the curve of 1.0 indicates perfect discrimination, whereas an area under the curve of 0.5 represents chance discrimination. The method of DeLong et al (19) was used to determine statistically significant differences among AUROCs.

Statistical analyses were performed using commercially available software (JMP Version 5.11, SAS Institute, Cary, NC; and SPSS 11.0.2, Chicago, IL).

RESULTS

The age, sex, average IOP, BCVA, central corneal thickness (CCT), mean deviation (MD), and corrected loss variance (CLV) of the visual field test nearest to the imaging date are presented in Table III. There was a statistically significant difference in age between glaucoma patients and healthy subjects (t-test, $p<0.001$). Sex, BCVA, and CCT were not significantly different between the two experimental groups (t-tests, $p=0.61$, $p=0.08$, and $p=0.18$, respectively). Average IOP (SD) of glaucoma eyes at the time of imaging was 20.1 (6.6) mm Hg. Average maximum IOP was 28.2 (8.7) mm Hg. Average IOP (SD) of the healthy eyes at the time of imaging was 13.8 (3.1) mm Hg.

The stage of visual field defects for each patient was determined according to the Brusini classification system (16, 18). Among OAG eyes, 19 (51%) patients were classified as having early glaucomatous loss (Stage 1 of the GSS) and 18 (49%) subjects had moderate glaucomatous loss (Stage 2 and 3). Average visual field MD (SD) for OAG and healthy eyes were 3.04 (5.02) dB and 0.19 (2.54) dB, respectively (t-test, $p<0.001$).

Average CLV (SD) for OAG and healthy eyes were 11.77 (8.09) dB^2 and 1.11 (0.87) dB^2 (t-test, $p<0.001$).

Statistically significant differences between experimental groups were found for all parameters except symmetry (t-test, $p=0.17$) and superior integral (t-test, $p=0.02$).

Table IV presents the mean RNFL values of the GDx parameters for OAG and healthy controls.

Statistically significant differences between groups were found for 5 of 12 parameters. Parameters that were not significantly different between groups (by t-test) were mean RNFL thickness ($p=0.38$), disk area ($p=0.48$), cup area ($p=0.01$), rim area ($p=0.02$), height variation contour ($p=0.02$), rim volume ($p=0.39$), and RNFL cross sectional area ($p=0.90$). Table V presents the mean disk topography values of the RTA parameters for OAG and healthy eyes. The AUROCs and sensitivities at fixed specificities for discriminating between glaucomatous and healthy eyes for GDx and RTA parameters are shown in Table VI. For GDx, ROC curve areas ranged from 0.58 (symmetry) to 0.91 (the number). The AUROC for the number was significantly greater than for all other GDx parameters (method of DeLong, $p<0.05$). For RTA, the AUROC ranged from 0.45 (RNFL cross sectional area) to 0.79 (mean cup depth). The AUROC for mean cup depth (0.79) was significantly greater than for disk area (0.53), rim volume (0.61), and RNFL cross sectional area (0.45) (method of DeLong,

p<0.05). The AUROC for GDx the number was significantly greater than the AUROC for RTA measured mean cup depth and all other RTA parameters (method of DeLong, p<0.05).

The AUROC for GDx the number was significantly larger (method of DeLong, p<0.05) than the AUROC from RTA mean cup depth. Figure 1 compares AUROCs for GDx the number and RTA mean cup depth.

DISCUSSION

Based on AUROC curves analyses, our results suggest that GDx can more successfully discriminate between glaucomatous eyes and healthy eyes than RTA. The largest AUROCs for GDx and RTA were 0.91 and 0.79, respectively. In addition, sensitivity at ≥80% and ≥95% specificity, for the parameter with the highest sensitivity for each instrument, was considerably higher for GDx than RTA (Tab. VI). Previously reported AUROCs for GDx range from 0.79 to 0.94 (20-22). In studies that included early to moderate glaucoma, sensitivities ranged from 33 to 81% at high fixed specificities of 90% (22, 23). These results are comparable to our results using GDx with fixed corneal compensation. Although a newer generation GDx currently is available, the GDx VCC (with variable corneal compensation) that incorporates a subject-specific variable corneal polarization axis and magnitude compensator, the earlier version of the GDx currently is used in many clinics. In addition, much longitudinal data has been collected that likely will appear in future articles to assess the ability of scanning laser polarimetry in general to pre-

TABLE III - CHARACTERISTICS OF THE STUDY POPULATION

	OAG (n=37)	Normal (n=34)	p Value*
Age, yr	63.5 (10.0)	52.2 (16.1)	<0 .001
Gender, F/M	24/13	24/10	0.61
Average IOP, mmHg	20.1 (6.6)	13.8 (3.1)	<0.0001
BCVA	20/25	20/20	0.08
CCT, µm	563.8 (33.2)	573.8 (28.5)	0.18
MD, dB	3.04 (5.02)	0.19 (2.54)	<0.0001

Data are given as mean (SD)
*t-Test
OAG = Open angle glaucoma; IOP = Intraocular pressure; BCVA = Best-corrected visual acuity; CCT = Central corneal thickness; MD = Mean deviation

TABLE IV - RETINAL NERVE FIBER LAYER (RNFL) MEASUREMENTS IN GLAUCOMA PATIENTS AND NORMAL CONTROLS USING GDx NERVE FIBER ANALYZER WITH FIXED CORNEAL COMPENSATION

Parameter	OAG (n=37)	Normal (n=34)	p Value*
Number	62.5 (22.7)	24.6 (15.4)	<0.0001
Symmetry†	0.09 (0.05)	0.08 (0.06)	0.17
Superior ratio	1.66 (0.29)	2.15 (0.42)	<0.0001
Inferior ratio	1.69 (0.33)	2.19 (0.40)	<0.0001
Superior/nasal ratio	1.55 (0.20)	1.88 (0.35)	<0.0001
Maximal modulation	0.82 (0.31)	1.30 (0.40)	<0.0001
Ellipse modulation	1.55 (0.60)	2.21 (0.77)	0.0001
Average thickness	55.6 (12.2)	65.3 (13.7)	0.002
Ellipse average	56.7 (12.7)	68.2 (13.9)	<0.0001
Superior average	61.2 (13.8)	75.2 (15.0)	<0.0001
Inferior average	63.4 (14.7)	80.1 (16.7)	<0.0001
Superior integral	0.18 (0.05)	0.21 (0.04)	0.02

Data are given as mean (SD)
*t-Test; after Bonferroni correction a p value of no more than 0.002 was considered statistically significant
†Because symmetry is calculated as the superior to inferior RNFL thickness ratio, the analysis was conducted on the absolute value of symmetry – 1, to represent the distance from perfect symmetry monotonically
OAG = Open angle glaucoma

TABLE V - OPTIC DISK TOPOGRAPHY OF GLAUCOMA PATIENTS AND NORMAL CONTROLS USING THE RETINAL THICKNESS ANALYZER (RTA)

Parameter	OAG (n=37)	Normal (n=34)	p Value*
Mean RNFL thickness	0.14 (0.14)	0.17 (0.09)	0.38
Disk area	2.79 (0.69)	2.69 (0.41)	0.48
Cup area	1.57 (0.71)	1.12 (0.72)	0.01
Cup/disk area ratio	0.61 (0.05)	0.41 (0.04)	<0.001
Rim area	1.10 (0.88)	1.57 (0.76)	0.02
Cup volume	0.49 (0.37)	0.24 (0.26)	<0.001
Rim volume	0.23 (0.29)	0.29 (0.26)	0.39
Mean cup depth	0.27 (0.10)	0.17 (0.08)	<0.0001
Maximum cup depth	0.67 (0.18)	0.52 (0.17)	<0.001
Cup shape measure	-0.12 (0.09)	-0.20 (0.09)	<0.001
Height variation contour	0.53 (0.25)	0.39 (0.21)	0.02
RNFL cross section area	0.85 (0.98)	0.82 (0.66)	0.90

Data are given as mean (SD)
*t-Test; after Bonferroni correction a p value of no more than 0.002 was considered statistically significant
OAG = Open angle glaucoma; RNFL = Retinal nerve fiber layer

TABLE VI - AREAS UNDER THE RECEIVER OPERATING CHARACTERISTICS (ROC) CURVES AND SENSITIVITIES AT FIXED SPECIFICITIES

GDx parameter	ROC (SE)	Sensitivity at ≥80% specificity	Sensitivity at 95% specificity
Number	0.91 (0.03)	85/84	73/95
Symmetry*	0.58 (0.07)	29/81	14/95
Superior ratio	0.83 (0.07)	68/84	53/95
Inferior ratio	0.84 (0.06)	68/81	53/95
Superior/nasal ratio	0.79 (0.06)	74/81	47/95
Maximal modulation	0.82 (0.05)	68/81	53/95
Ellipse modulation	0.74 (0.06)	61/81	41/95
Average thickness	0.72 (0.02)	41/81	18/95
Ellipse average	0.73 (0.02)	47/84	12/95
Superior average	0.76 (0.02)	50/81	21/95
Inferior average	0.79 (0.02)	53/84	27/95
Superior integral	0.68 (0.08)	47/81	5/95
RTA parameter	**ROC (SE)**	**Sensitivity at ≥80% specificity**	**Sensitivity at ≥95% specificity**
Mean RNFL thickness	0.62 (0.08)	29/81	2/95
Disk area	0.53 (0.05)	8/81	8/95
Cup area	0.68 (0.08)	38/81	14/96
Cup/disk area ratio	0.70 (0.09)	47/81	15/95
Rim area	0.68 (0.08)	38/81	5/96
Cup volume	0.74 (0.06)	70/81	12/97
Rim volume	0.61 (0.07)	24/81	5/96
Mean cup depth	0.79 (0.08)	61/82	33/95
Maximum cup depth	0.72 (0.08)	55/80	21/97
Cup shape measure	0.77 (0.07)	55/84	36/97
Height variation contour	0.70 (0.08)	55/83	27/95
RNFL cross section area	0.45 (0.09)	9/81	3/95

*Because symmetry is calculated as the superior to inferior retinal nerve fiber layer (RNFL) thickness ratio, the analysis was conducted on the absolute value of symmetry – 1, to represent the distance from perfect symmetry monotonically

dict glaucomatous conversion and progression (24, 25). Our results, although not based on GDx VCC technology, provide encouraging results for the use of scanning laser polarimetry for the diagnosis of glaucoma in general. Additionally, our results provide new information about the ability of RTA technology in the diagnosis of glaucoma and suggest that RTA optic disk topography measurement is not yet acceptable as a new alternative for scanning laser polarimetry RNFL measurements.

We agree with previous reports that VCC technology can improve the ability of SLP to discriminate between healthy and glaucomatous eyes (5, 26, 27). However, several of the reported improvements using GDx VCC are slight (26, 28), and it has been shown that the ratio and modulation parameters obtained using GDx VCC are similar to those obtained using GDx with fixed corneal compensation (26 27) (although thickness parameters provide better glaucoma versus healthy discrimination using VCC). In addition, the current GDx VCC retains some limitations. One observed concern is the presence of atypical scan patterns that have been identified in some subjects that suggest areas of artificially high retardation (i.e., thick RNFL thickness) (5).

The poor classification results associated with most RTA optic disk topography measurements in the current study might be the result of several factors. First, the RTA uses slit lamp technology to obtain cross sections of the respective tissue by reflection, which may provide non-optimal image quality, and thus inaccurate measurements in some eyes (29). In addition, non-optimal image quality could lead to difficulty in subjectively defining the contour line used to calculate most RTA topographic parameters, thus compromising measurement accuracy and therefore diagnostic precision. The Heidelberg Retina Tomograph, which uses confocal scanning technology to obtain retinal height measurements used to depict optic disk topography and which also uses a subjectively defined reference plane, has been shown to have similar glaucoma detection ability as the GDx (20, 26, 30). Therefore, it is possible that RTA technology is not yet well developed enough for subjective reference plane-based optic disk topography measurement. One further concern might be the required interpolation used by the RTA to produce a surface map of the optic disk. It is possible that this strategy could overlook defects or changes in disk topography.

Only one study (12) reported AUROCs using RTA posterior pole measurements in the diagnosis of glaucoma. AUROCs for posterior pole indices ranged from 0.82 to 0.97. The sensitivity at fixed specificity was highest to differentiate between normal and glaucoma by using the parameter perifoveal minimum thickness (sensitivity = 95% at specificity = 90%).

One limitation of the current study is limited sample size that could decrease the generalization of the results and mask small but significant differences between groups observable in large population studies. In addition, healthy participants and patients with glaucoma differed significantly in age. Although age might have affected quality of images, each image from both instruments was reviewed for good quality by an experienced examiner. Therefore, influence on the results of the study by poor quality images is unlikely. It is furthermore not likely that age affected discrimination for either instrument because we examined the association between age and each parameter from both instruments in the healthy eyes using linear regression. Only the association between age and GDx number was significant ($r^2 = 0.13$, $p=0.04$), indicating that age had little effect on the measurements from these instruments (in our population with a limited age range). Moreover, the purpose of this study was to compare the discriminative ability of GDx and RTA in the same population. Therefore, any difference in age likely affected measurements for each instrument similarly. Because age was significantly associated with GDx number, we recalculated the AUROC for this parameter while including age as a discriminant factor. The AUROC changed minimally from 0.91 to 0.92. Overall, topographic RTA parameters were less able to discriminate between healthy and glaucomatous eyes than GDx RNFL parameters. Despite the use of GDx with fixed corneal compensation, discrimination was significantly better using GDx compared to RTA, suggesting that currently available RTA optic disk analysis software likely cannot replace GDx RNFL analysis software for glaucoma diagnosis.

The authors have no financial interest in any of the devices used in this article. No financial support was provided.

Reprint requests to:
Esther M. Hoffmann, MD
University of Mainz
Dept. of Ophthalmology
Langenbeckstrasse, 1
55101 Mainz, Germany
ehoffman@mail.uni-mainz.de

REFERENCES

1. Wilson MR, Khanna S. The value of different screening techniques for glaucoma. Curr Opin Ophthalmol 1994; 5: 69-75.
2. Weinreb RN. Laser scanning tomography to diagnose and monitor glaucoma. Curr Opin Ophthalmol 1993; 4: 3-6.
3. Weinreb RN, Shakiba S, Zangwill L. Scanning laser polarimetry to measure the nerve fiber layer of normal and glaucomatous eyes. Am J Ophthalmol 1995; 119: 627-36.
4. Weinreb RN, Zangwill LM. Imaging technologies for assessing neuroprotection in glaucomatous optic neuropathy. Eur J Ophthalmol 1999; 9 (Suppl.): S40-3.
5. Medeiros FA, Zangwill LM, Bowd C, Weinreb RN. Comparison of the GDx VCC scanning laser polarimeter, HRT II confocal scanning laser ophthalmoscope, and Stratus OCT optical coherence tomograph for the detection of glaucoma. Arch Ophthalmol 2004; 122: 827-37.
6. Asrani S, Zeimer R, Goldberg MF, Zou S. Application of rapid scanning retinal thickness analysis in retinal diseases. Ophthalmology 1997; 104: 1145-51.
7. Asrani S, Zou S, d'Anna S, Vitale S, Zeimer R. Noninvasive mapping of the normal retinal thickness at the posterior pole. Ophthalmology 1999; 106: 269-73.
8. Zeimer R, Shahidi M, Mori M, Zou S, Asrani S. A new method for rapid mapping of the retinal thickness at the posterior pole. Invest Ophthalmol Vis Sci 1996; 37: 1994-2001.
9. Weinreb RN. Evaluating the retinal nerve fiber layer in glaucoma with scanning laser polarimetry. Arch Ophthalmol 1999; 117: 1403-6.
10. Hoh ST, Greenfield DS, Liebmann JM, et al. Factors affecting image acquisition during scanning laser polarimetry. Ophthalmic Surg Lasers 1998; 29: 545-51.
11. Choplin NT, Lundy DC. The sensitivity and specificity of scanning laser polarimetry in the detection of glaucoma in a clinical setting. Ophthalmology 2001; 108: 899-904.
12 Tanito M, Itai N, Ohira A, Chihara E. Reduction of posterior pole retinal thickness in glaucoma detected using the Retinal Thickness Analyzer. Ophthalmology 2004; 111: 265-75.
13. Martinez de la Casa JM, Garcia Feijoo J, Castillo Gomez A, Garcia Sanchez J. [Correlations between retinal thickness analyzer (RTA) and confocal scanning laser tomography (HRT) in optic disk analysis.] Arch Soc Esp Oftalmol 2004; 79: 21-5.
14. Itai N, Tanito M, Chihara E. Comparison of optic disk topography measured by Retinal Thickness Analyzer with measurement by Heidelberg Retina Tomograph II. Jpn J Ophthalmol 2003; 47: 214-20.
15. Flammer J, Drance SM, Augustiny L, Funkhouser A. Quantification of glaucomatous visual field defects with automated perimetry. Invest Ophthalmol Vis Sci 1985; 26: 176-81.
16. Brusini P. Clinical use of a new method for visual field damage classification in glaucoma. Eur J Ophthalmol 1996; 6: 402-7.
17. Zulauf M, LeBlanc RP, Flammer J. Normal visual fields measured with Octopus-Program G1. II. Global visual field indices. Graefes Arch Clin Exp Ophthalmol 1994; 232: 516-22.
18. Kocak I, Zulauf M, Bergamin O. Evaluation of the Brusini glaucoma staging system for typing and staging of perimetric results. Ophthalmologica 1998; 212: 221-7.
19. DeLong ER, DeLong DM, Clarke-Pearson DL. Comparing the areas under two or more correlated receiver operating characteristic curves: a nonparametric approach. Biometrics 1988; 44: 837-45.
20. Greaney MJ, Hoffman DC, Garway-Heath DF, Nakla M, Coleman AL, Caprioli J. Comparison of optic nerve imaging methods to distinguish normal eyes from those with glaucoma. Invest Ophthalmol Vis Sci 2002; 43: 140-5.
21. Bowd C, Zangwill LM, Berry CC, et al. Detecting early glaucoma by assessment of retinal nerve fiber layer thickness and visual function. Invest Ophthalmol Vis Sci 2001; 42: 1993-2003.
22. Weinreb RN, Zangwill L, Berry CC, Bathija R, Sample PA. Detection of glaucoma with scanning laser polarimetry. Arch Ophthalmol 1998; 116: 1583-9.
23. Sinai MJ, Essock EA, Fechtner RD, Srinivasan N. Diffuse and localized nerve fiber layer loss measured with a scanning laser polarimeter: sensitivity and specificity of detecting glaucoma. J Glaucoma 2000; 9: 154-62.
24. Mohammadi K, Bowd C, Weinreb RN, Medeiros FA, Sample PA, Zangwill LM. Retinal nerve fiber layer thickness measurements with scanning laser polarimetry predict glaucomatous visual field loss. Am J Ophthalmol 2004; 138: 592-601.
25. Hollo G, Szabo A, Vargha P. Scanning laser polarimetry versus frequency-doubling perimetry and conventional threshold perimetry: changes during a 12-month follow-up in preperimetric glaucoma. A pilot study. Acta Ophthalmol Scand 2001; 79: 403-7.
26. Weinreb RN, Bowd C, Zangwill LM. Glaucoma detection using scanning laser polarimetry with variable corneal polarization compensation. Arch Ophthalmol 2003; 121: 218-24.
27. Choplin NT, Zhou Q, Knighton RW. Effect of individualized compensation for anterior segment birefringence on retinal nerve fiber layer assessments as determined by scanning laser polarimetry. Ophthalmology 2003; 110: 719-25.
28. Greenfield DS, Knighton RW, Feuer WJ, Schiffman JC, Zangwill L, Weinreb RN. Correction for corneal polarization axis improves the discriminating power of scanning laser polarimetry. Am J Ophthalmol 2002; 134: 27-33.
29. Polito A, Shah SM, Haller JA, et al. Comparison between retinal thickness analyzer and optical coherence tomography for assessment of foveal thickness in eyes with macular disease. Am J Ophthalmol 2002; 134: 240-51.
30. Zangwill LM, Bowd C, Berry CC, et al. Discriminating between normal and glaucomatous eyes using the Heidelberg Retina Tomograph, GDx Nerve Fiber Analyzer, and Optical Coherence Tomograph. Arch Ophthalmol 2001; 119: 985-93.